International Journal of Thermophysics, Vol. 8, No. 1, 1987

Measurement of Infrared Absorption of Some Oxides in Connection with the Radiative Transfer in Porous and Fibrous Materials

F. Cabannes[1] **and D. Billard**[1]

Received February 26, 1986

The radiative heat transfer in porous and fibrous materials depends on the infrared absorption and scattering properties of the materials. The infrared absorption can be obtained by transmission measurements in single crystals. It is shown in the case of Al_2O_3 and MgO that the analysis of absorption data as a function of temperature gives the possibility of decomposing the lattice absorption coefficient in its different multiphonon contributions. The study of multiphonon components is necessary to understand as well as to predict the frequency and temperature behavior of the lattice absorption in materials. Measurements performed on TiO_2 and ZrO_2 also are reported; it is observed that electronic effects considerably enhance the absorption level at high temperatures. From diffuse reflection measurements on a scattering sample, the ratio of absorption and scattering can be obtained. So experimental data can be used to calculate the radiant flux. Several models have been proposed, based on isotropic and anisotropic approximations. They involve the absorption coefficient σ_a, the scattering coefficient σ_s, the backscattered fraction factor b, and a phase function parameter a_1. Due to the approximations on which the models are based, the calculated values of the radiant heat flux show large differences (as large as 30%), whatever the accuracy of the values of optical parameters which are used. It appears worthy to use the experimental data on σ_a and σ_s, which can be obtained from transmission and diffuse reflection measurements.

KEY WORDS: dielectric function; infrared radiation; lattice absorption; multiphonon absorption; oxides; radiative transfer.

[1] Université d'Orléans et Centre de Recherches sur la Physique des Hautes Températures du CNRS, 45071 Orléans-cedex, France.

0195-928X/87/0100-0097$05.00/0

1. INTRODUCTION

The investigation of radiative transfer in fiber insulation and porous ceramics involves the knowledge of the infrared properties of the medium: absorption and scattering. The infrared absorption in transparent solids has to be investigated also for solving pyrometry problems. Moreover, in recent years, the advance of high-power lasers and fiber guides required more attention to the absorption in ionic solids.

The aim of this paper is (a) to summarize the research on infrared absorption which was carried out at the Centre de Recherche sur la Physique des Hautes Températures (CRPHT) in Orléans, France, and (b) to review some aspects of the radiation heat transfer in absorbing and scattering media.

The infrared absorption was measured over wide spectral and temperature ranges, as wide as possible, which allows a detailed analysis of multiphonon absorption, as described below.

2. EXPERIMENTAL TECHNIQUES FOR INFRARED ABSORPTION MEASUREMENT

The experimental techniques include transmission measurements, sample temperature measurements, and heating techniques.

The optical setup for transmission measurements is well known. The spectrometer is either a conventional one for measurements in the near-infrared (Fig. 1) or a Fourier transform scanning (FTS) spectrometer for the far-infrared (Fig. 2).

2.1. Transmission Measurement

Above room temperature, the thermal radiation of samples disturbs the transmission measurements. To eliminate the thermal emission in measurements using a conventional spectrometer, the infrared beam is usually chopped ahead of the sample so that its thermal emission is not modulated and thus it is not detected.

By using a FTS spectrometer, it is more difficult to eliminate the emission of the sample. However, this kind of spectrometer has two advantages: a very wide spectral range (2500–20 cm^{-1}) and very fast measurements. Because any chopper cannot be put into rapid-scan interferometers, the sample acts as a second source producing a negative contribution, which adds to the signal coming from the infrared source. This difficulty can be overcome in interferometers such as the Bruker system, by means of a slight misalignment of the beams inside the interferometer com-

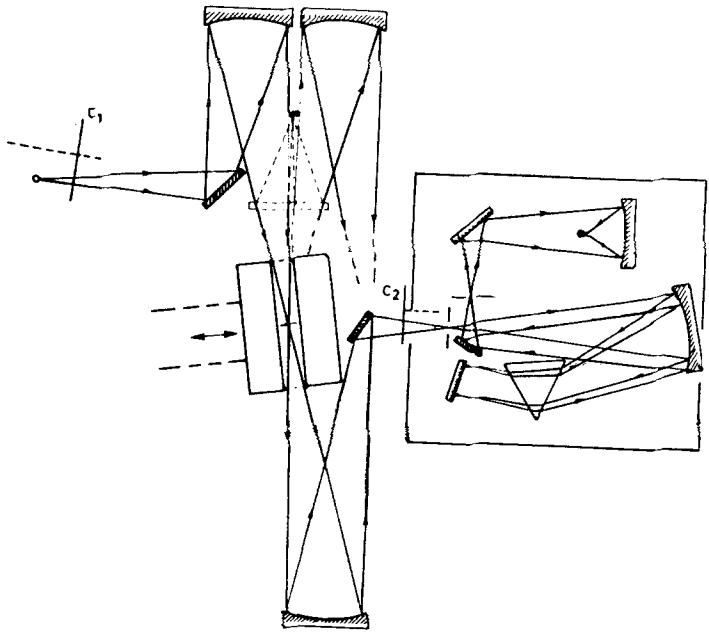

Fig. 1. Optical setup for transmission measurements (using a conventional spectrometer). C1, chopper for transmittance measurement; C2, chopper for temperature measurement by means of the thermal emission of the sample.

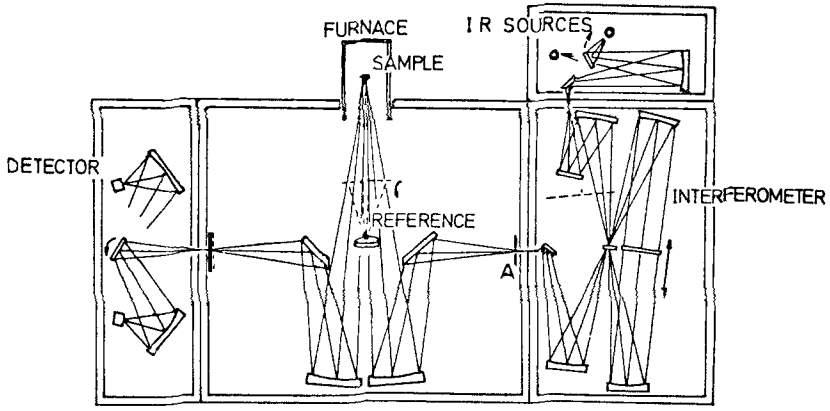

Fig. 2. Optical setup for reflection measurements using a FTS spectrometer. An easy modification leads to transmission measurements [1].

partment [1]. The beams coming from the source and from the sample are separated, then an aperture positioned at an intermediate focus allows the source signal to reach the detector, while the sample thermal signal is masked.

2.2. Temperature Measurement

With the conventional spectrometer, the temperature of samples was determined by measurement of their thermal emission. To do that, a removable chopper is put between the sample and the detector. One selects a frequency at which the crystal emits like a blackbody, i.e., where the reflectivity is minimum. For most of the ionic oxides this frequency is between 800 and 1000 cm^{-1}. The detector is calibrated with a blackbody. In the case of the FTS spectrometer, temperature measurements were carried out by means of a thermocouple, which is calibrated at the temperature of a known phase transition such as the α–β phase transition of quartz.

2.3. Heating Techniques

Two very different heating techniques were used.

Thin oxide crystals can be heated up to their melting temperature by a CO_2 laser beam. A 600-W laser working in a continuous regime was used. The laser heating is convenient when an accurate temperature control is not needed.

Small conventional electrical furnaces were used to heat samples below 1400 K. Sample temperatures of the order of 2100 K were obtained with a "zirconia" furnace. Such a furnace is useful when the large thickness of the sample does not allow the heating by a laser beam. The so-called zirconia furnace is an electrical furnace built in the CRPHT.[2] Several types are used for the following studies: sintering, electrical conductivity measurement, high-temperature creep investigation, and thermal decomposition of water and CO_2.

The smallest furnace (Fig. 3) is needed for infrared transmission measurements. It has the following characteristics [2].

Size of the hot zone: diameter, 20 mm; length, 20 mm

Temperature gradient when the furnace is open (Fig. 4)

Electrical power: 1200 W

External size: $100 \times 100 \times 120$ mm

[2] Centre de Recherches sur la Physique des Hautes Températures, CNRS, Orléans, France.

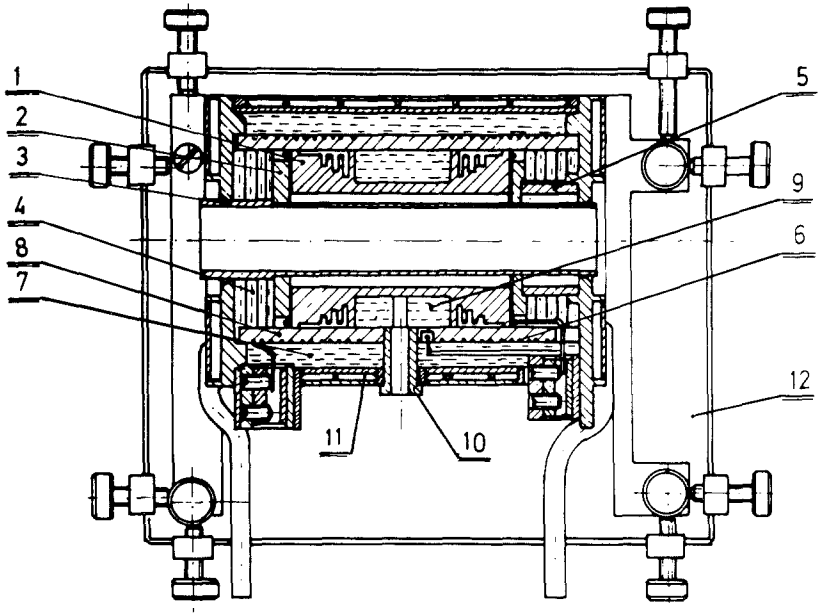

Fig. 3. Cross-sectional diagram of the zirconia furnace [2]. (1) Heater made of zirconia ceramics; (4, 7, 9) zirconia felt thermal insulation; (6) platinum preheating wire; (11) water-cooled jacket.

The heating element is machined of porous zirconia ceramics and placed inside a kanthal preheating furnace. The furnace is designed in such a way that the temperature of the kanthal wire is 900°C and the electrical contact on the zirconia is not heated above 1300°C when the hottest zone is at 1800°C. Since zirconia ceramics are brittle, the furnace is sensitive to thermal shock and the heating rate should not exceed $400°C \cdot h^{-1}$.

3. TRANSMISSION EXPERIMENTAL DATA

As an example the infrared transmittance of aluminium oxide single crystal (corundum) is shown in Fig. 5. The temperature is in the range 77–2035 K and the thickness of samples is between 0.167 and 10 mm.

The infrared reflectivity has been studied extensively in the CRPHT and elsewhere. Thus, the absorption coefficient k can be calculated from reflectivity data R and transmission data τ, according to the usual expression:

$$\tau = (1-R)^2 \exp(-kd)/[1-R^2 \exp(-2kd)] \quad (1)$$

where d is the sample thickness.

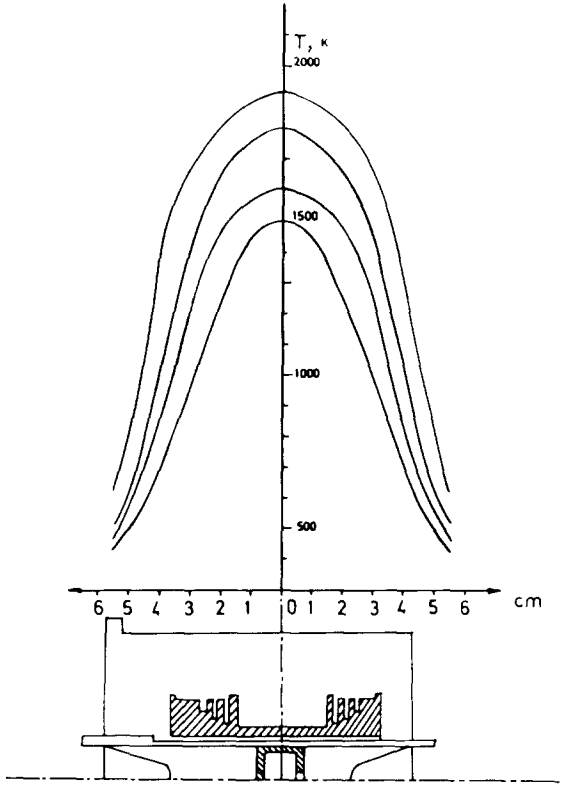

Fig. 4. Axial temperature distribution in the furnace.

The results are reported either as a function of frequency or as a function of temperature. The frequency dependence in the near-infrared is shown in Figs. 6, 7, and 8, for corundum (ordinary ray) between 77 and 2035 K [3], for magnesium oxide [2], and for yttria-stabilized cubic zirconium oxide [4]. The spectra display weak structural features, which progressively disappear with increasing temperature. Moreover, the absorption versus frequency curves exhibit a nearly exponential decrease at a fixed temperature. All this is typical of multiphonon edge absorption occurring in ionic crystals [5].

The simplest way proposed to analyze the temperature dependence of the infrared edge absorption is [5]

$$K = K_0[n(\omega_0)+1]^{\omega/\omega_0}[n(\omega)+1]^{-1}\exp(-A\omega/\omega_0) \tag{2}$$

where $n(\omega)$ is the Bose–Einstein function and ω_0 is a temperature-depen-

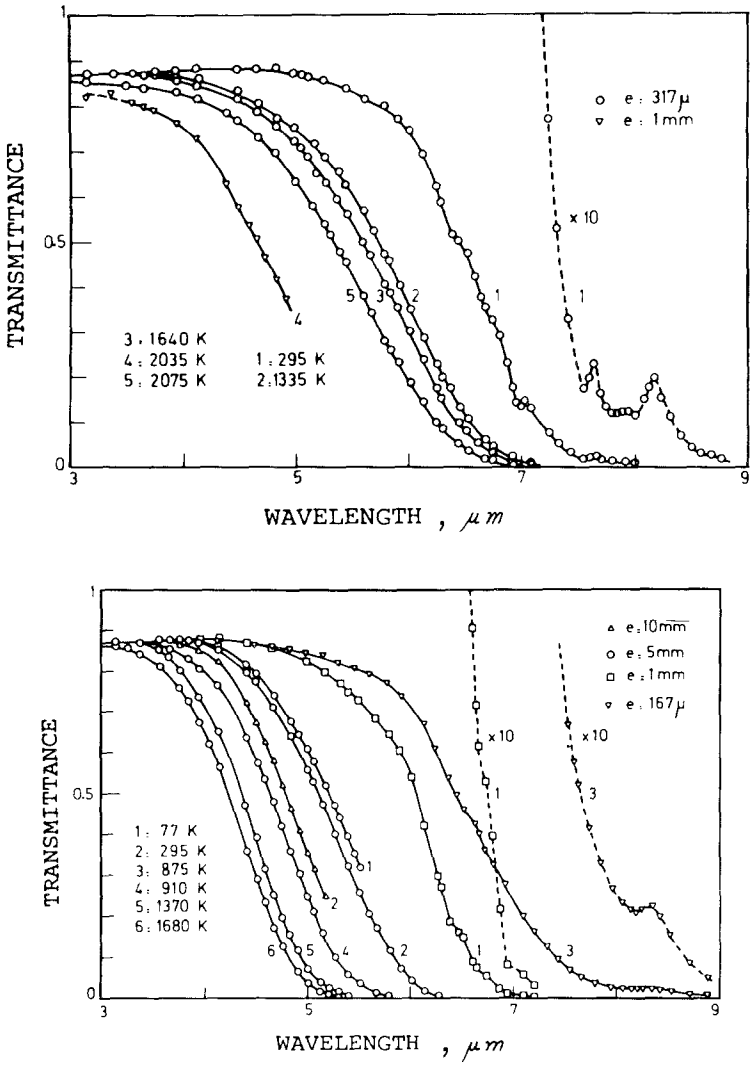

Fig. 5. Measured transmittance of corundum (ordinary ray) at selected temperatures in the near-infrared (e, thickness of samples) [3].

dent average optical phonon frequency, which can reasonably be considered as linearly varying with temperature, in the form

$$\omega_0 - \omega_{00} = -\gamma \omega_{00} T \tag{3}$$

The best fit of Eqs. (2) and (3) to the data for cubic zirconium oxide over the full range of available temperatures and frequencies is obtained for

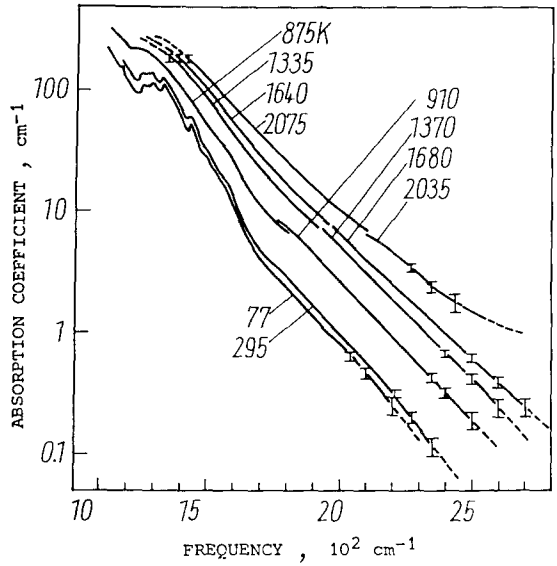

Fig. 6. Experimental frequency dependence of the absorption coefficient of corundum (ordinary ray) in the near-infrared between 77 and 2075 K [6].

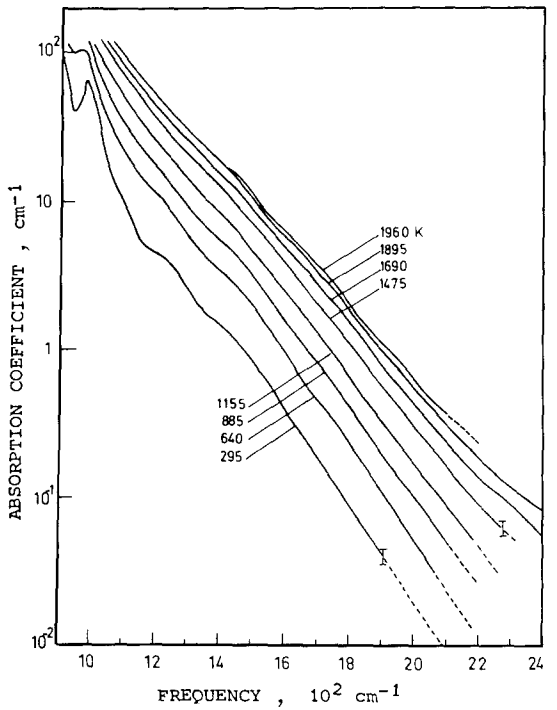

Fig. 7. Experimental frequency dependence of the absorption coefficient of MgO in the near-infrared between 295 and 1960 K [2].

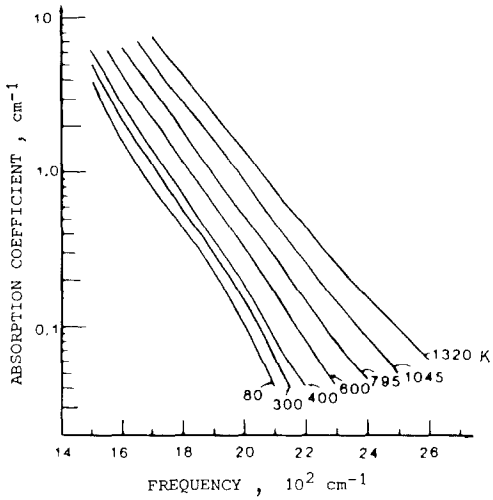

Fig. 8. Experimental frequency dependence of the absorption coefficient of cubic zirconia in the near-infrared between 80 and 1320 K [4].

$\omega_{00} = 550\ \text{cm}^{-1}$, which is consistent with fundamental infrared and Raman data and implies that the present absorption measurements span the three- to five-phonon regime, since the frequency range extends to $2600\ \text{cm}^{-1}$.

Thus, from Eq. (2) the temperature dependence of the infrared edge absorption can be calculated, providing a qualitatively correct description of experimental data [5].

In the case of corundum and magnesium oxide, a more complete analysis of absorption has been obtained by investigating each contribution of the n-phonon interaction processes, separately. The n-phonon contributions to absorption are directly separated by means of an analysis of the temperature dependence of data in the high-temperature range [6]. In this way, each contribution can be discussed in detail by comparison with predictions of a theoretical model. Such a complete analysis cannot be achieved for zirconium oxide, because electronic effects disturb the multiphonon processes at high temperatures, as seen below.

4. ANALYSIS OF MULTIPHONON ABSORPTION

In this section the analysis developed by Billard et al. is briefly presented. The absorption coefficient can be expressed, in the transmission region, as

$$K = \omega \cdot \varepsilon''/c(\varepsilon')^{1/2} \tag{4}$$

where ω is the frequency of the incident photon, $\varepsilon = \varepsilon' - i\varepsilon''$ is the complex dielectric function, and c is the light velocity.

In the classical dispersion theory, the dielectric function is expressed in the form

$$\varepsilon = \varepsilon_\infty + \sum_j \Delta\varepsilon_j \Omega_j^2/(\Omega_j^2 - \omega^2 - i\omega\gamma_j) \tag{5}$$

where $\Delta\varepsilon_j$, Ω_j, and γ_j are respectively the oscillator strength, the resonance frequency, and the damping of the fundamental vibration mode j (transverse optical mode).

Equation (5) is a good approximation in the region of fundamental modes for describing the reflection spectrum [7]. At a fixed temperature, the damping γ_j can be approximated as independent of frequency in the vicinity of $\omega = \Omega_j$. The quantity γ_j statistically accounts for all anharmonic couplings which relax the mode j, therefore it increases with temperature.

Infrared radiation is transmitted far away from the resonance frequencies, at high and low frequencies. The quantum theory of weakly anharmonic crystals postulates that the damping γ_j and the frequency Ω_j of a fundamental mode are not constant, but they are functions of frequency and of temperature:

$$\Omega_j^2 = \omega_j^2 + 2\omega_j[\delta\omega_j(T) + \Delta\omega_j(\omega, T)] \tag{6}$$

$$\gamma_j = 2\omega_j \Gamma_j(\omega, T)/\omega \tag{7}$$

Here the frequency shift $\Delta\omega_j(\omega, T)$ and the damping $\Gamma_j(\omega, T)$ are, respectively, the real and imaginary part of the phonon self-energy function of the fundamental mode j [1]:

$$P_j(\omega, T) = \Delta\omega_j(\omega, T) + i\Gamma_j(\omega, T) \tag{8}$$

The frequency shift $\delta\omega_j$ takes account of the mechanical effects of lattice thermal expansion.

It is easy to understand why Γ_j is frequency dependent. The fundamental vibration mode j, excited by an incident photon at the frequency ω, decays by anharmonic coupling with other phonon modes of the crystal. Absorption in the near-infrared ($\omega \gg \Omega_j$) is dominated by n-phonon summation interaction processes ($n \geqslant 2$) in which an incident photon leads to the final excitation of n phonons of frequencies ω_1, ω_2,..., ω_n, such as

$$\omega = \sum_{i=1,n} \omega_i \tag{9}$$

which is the energy conservation condition.

It is evident that the magnitude of Γ_j depends on the number of possible couplings, which is a function of ω, according to Eq. (9). In other words, Γ_j is related to the multiphonon densities of states of the crystal.

The infrared lattice absorption, resulting from the interaction of incident photons with phonon modes of the crystal, occurs via the excitation of fundamental polar modes as mentioned above (anharmonic mechanism) but also by direct coupling through the nonlinear electric moment (Lax–Burnstein mechanism). The contribution to the absorption coefficient of summation interactions involving n final phonons is described by an n-phonon absorption term K_n^+, so that in the near-infrared

$$K(T) = \sum_{n \geq 2} K_n^+ \tag{10}$$

K_n^+ is obtained from a quantum treatment of absorption. It can be schematically written as [2, 6]

$$K_n^+(\omega, T) = C_n(\omega) \sum_{Q_1, Q_2, \ldots, Q_n} [(N_1+1)(N_2+1)\cdots(N_n+1) - N_1 N_2 \cdots N_n] \cdot \delta(\omega - \omega_1 - \omega_2 \cdots - \omega_n) \tag{11a}$$

where δ represents the energy conservation, and N_i is the Bose–Einstein population factor for a phonon Q_i of frequency ω_i:

$$N_i = N_i(\omega, T) = [\exp(\hbar\omega_i/kT) - 1]^{-1} \tag{11b}$$

$C_n(\omega)$ is a coefficient of which the form is dependent on the nature of the absorption mechanism.

An usual assumption in the near-infrared is that the frequencies of n phonons excited in an interaction are dispersed on both sides of an average frequency ω/n. Then, as a whole, the absorption coefficient can be expressed in the simplified form

$$\begin{aligned} K(\omega, T) &= \sum_{n \geq 2} K_n^+(\omega, T) \\ &= \xi(T) \sum_{n \geq 2} K_n^+(\omega, 0)\{[N(\omega/n, T) + 1]^n - [N(\omega/n, T)]^n\} \end{aligned} \tag{12}$$

$\xi(T)$ accounts for lattice thermal expansion effects. The temperature dependence is dominated by phonon population terms, which exhibit for an n-phonon absorption at high temperatures a T^{n-1} typical behavior. The same temperature dependence (due to phonon populations) holds for the damping Γ_j (K and Γ_j are proportional in the anharmonic mechanism).

As shown in Fig. 9 for corundum and in Fig. 10 for magnesium oxide,

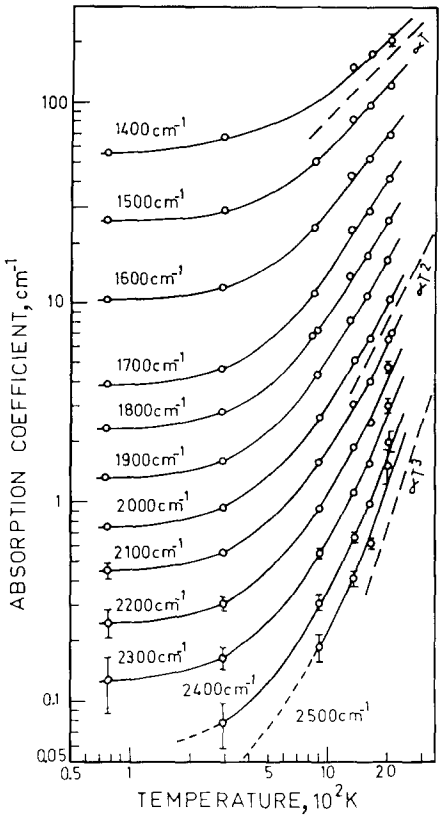

Fig. 9. Experimental (circles) and calculated (solid lines) temperature dependence of the absorption coefficient of corundum (ordinary ray) in the near-infrared [3].

Eq. (12) leads to a good fit of experimental absorption as a function of temperature. In addition, the different coefficients $K_n^+(\omega, 0)$ used to obtain the best agreement with data are distinguished. In other words, Eq. (12) allows one to realize a multiphonon decomposition of absorption. Thus, in the near-infrared analysis of Al_2O_3 and MgO (Figs. 9 and 10), summation absorption processes involving from two to five phonons have been determined [coefficient $K_n^+(\omega, 0)$ tabulated in Refs. 8 and 2. These results are consistent with theoretical predictions: in particular, it is well verified that n-phonon summation absorption processes vanish beyond $\omega = n\omega_M$, ω_M denoting the maximum phonon frequency ($\simeq 900\,cm^{-1}$ for Al_2O_3 and $730\,cm^{-1}$ for MgO), while $(n-1)$-phonon summation processes are

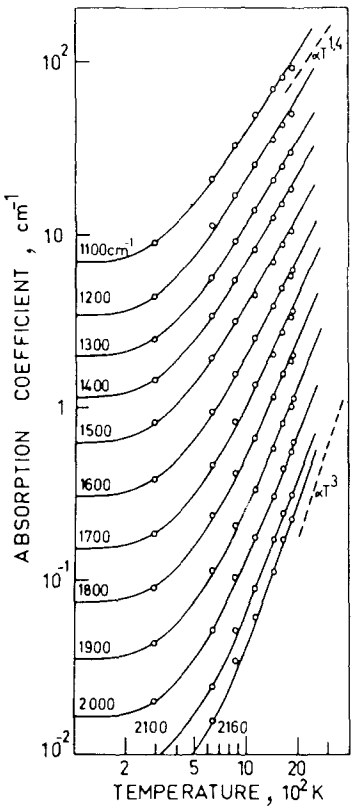

Fig. 10. Experimental (circles) and calculated (solid lines) temperature dependence of the absorption coefficient of MgO in the near-infrared [2].

predominant just below $n\omega_M$ [2, 3]. Considering only the high-temperature behavior of absorption, the succession of multiphonon processes, the order of which increases with frequency, is evident in Figs. 9 and 10.

However, a really quantitative study of absorption requires the use of a more complete model [based on Eq. (11)], in which all the temperature-implicit dependences must be taken into account (thermal expansion effects, phonon frequency shifts). In addition, it is convenient to introduce explicitly in the model the multiphonon densities of states of the crystal.

Such a study has been made by Billard et al. [6], who calculated phonon densities of states of orders 2 to 4 and could discuss the frequency behavior of multiphonon absorption terms. An essential consequence is the

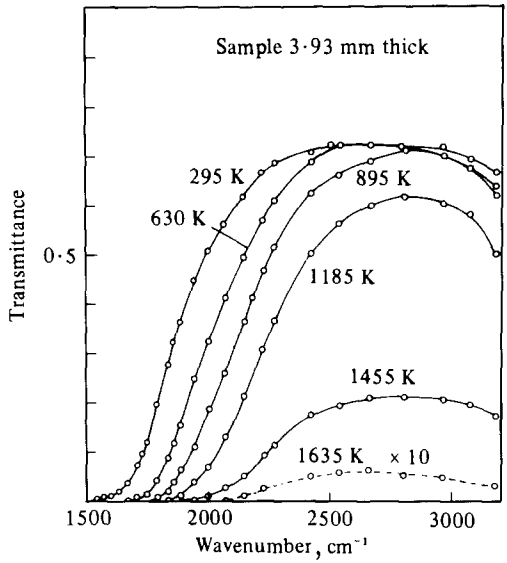

Fig. 11. Measured transmittance of rutile (ordinary ray) in the near-infrared between 295 and 1635 K [10].

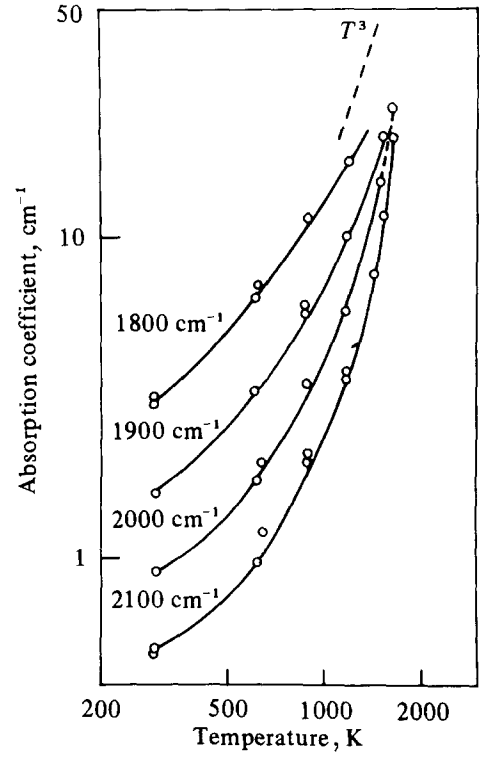

Fig. 12. Experimental temperature dependence of the absorption coefficient of rutile (ordinary ray) in the near-infrared [10]. Compare to Figs. 9 and 10.

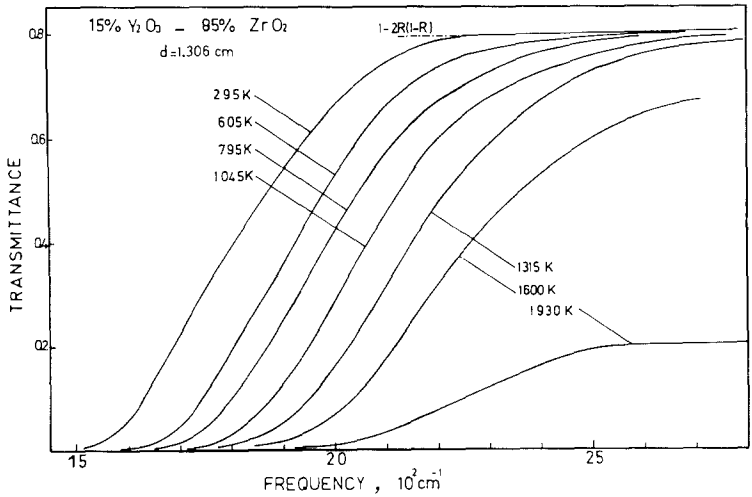

Fig. 13. Measured transmittance of yttria-stabilized cubic zirconium oxide in the near-infrared between 295 and 1930 K [9].

possibility of predicting the temperature and frequency dependence of lattice absorption in materials.

It should be emphasized that the multiphonon analysis is valid as long as the absorption may be interpreted in terms of lattice absorption alone. In the case of rutile, the transmission data show a sharp increasing of absorption at high frequencies (above 2000 cm^{-1}) when the temperature becomes higher than 1200 K (Figs. 11 and 12). It is probable that this additional absorption is caused by electronic excitations. The same behavior is observed in stabilized zirconium oxide [9] (Fig. 13). Such electronic excitations could result from a nonstoichiometry or impurity effects.

4.1. Far-Infrared Absorption

The multiphon analysis can explain the far-infrared absorption as well as the near-infrared absorption. Billard et al. [11] carried out absorption measurements in the frequency range 20–350 cm^{-1} on corundum and magnesium oxide crystals. They obtained a very good agreement between the experimental data and the theoretical calculation based on two- and three-phonon difference interaction processes, as illustrated in Fig. 14. According to a method similar to the one described above for the near-infrared, it is the measurement on a wide temperature range which allows one to separate the two- and three-phonon contributions.

In conclusion, the analysis of multiphonon absorption is a powerful approach to predict the lattice absorption of some ionic crystals over wide

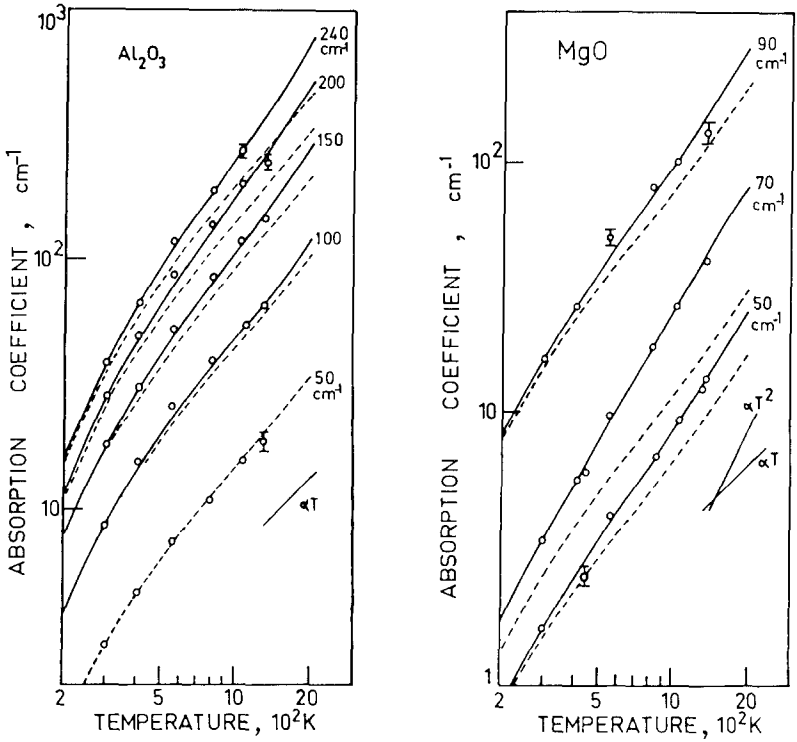

Fig. 14. Absorption coefficient of corundum (ordinary ray) and magnesium oxide vs temperature at selected frequencies in the far-infrared. Circles, experimental data; solid lines, theoretical calculations with two- and three-phonon difference processes; dashed lines, calculated contributions of two-phonon difference process alone [11].

frequency and temperature ranges, especially in the region of their thermal radiation between 1000 and 2000 K. The results of such an analysis are useful for computing the radiation heat transfer in absorbing media.

5. RADIATIVE HEAT TRANSFER IN ABSORBING AND SCATTERING MEDIA

Several models have been proposed to predict the heat transfer by radiation processes. All of them involve more or less drastic approximations. The absorption coefficient and scattering coefficient appear and they should be either computed or measured. Their values are more or less accurate. Therefore, it is useful to compare the different models in order to estimate what could be the accuracy needed.

5.1. Isotropic Scattering

The well-known model of Schuster and Schwarzchild (at the beginning of the century) leads to the expression of the radiant heat flux

$$q = -dM^0/d\tau = \sigma^0(T_1^4 - T_2^4)/\tau_0 \tag{13}$$

where τ_0 is the optical thickness and M^0 is the blackbody total emittance. From Eq. (13) the radiation thermal conductivity is written

$$k_r = 4\sigma^0 T^3/\sigma_e \tag{14}$$

where

$$\sigma_e = \sigma_a + \sigma_s \tag{15}$$

σ_a and σ_s are the absorption and scattering coefficient, respectively, and σ^0 is the Stephan constant.

This model is based on the simplest approximation. For one-dimensional energy transfer, it is assumed that the intensity is isotropic in the forward direction and that in the backward direction it has a different value but it is also isotropic.

As noted by Siegel and Howell [12], the same approximation was used by Milne in 1930 and by Eddington in 1959, but they used the isotropic approximation to calculate heat fluxes rather than intensities. Then they obtained the equation

$$q = -(4/3)\, dM^0/d\tau = 4\sigma^0(T_1^4 - T_2^4)/3\tau_0 \tag{16}$$

instead of Eq. (13). Equation (16) is identical to the Rosseland diffusion equation.

It should be emphasized that Eqs. (13) and (16) give two values of the flux, the ratio of which is 4/3.

5.2. Anisotropic Scattering

In fibrous materials used for thermal insulation, the scattering can be much more important than the absorption, in the heat transfer processes by radiation. The scattering by fine particles cannot be considered as isotropic, so the two-flux model was refined, at first by Larkin and Churchill [13].

Two refined models are presented below, following Tong and Tien [14]. The radiation transfer is calculated without coupling with conduction; the heat flux from conduction is added only after calculation.

5.3. Two-Flux (TF) Model

After introducing the two-flux and gray approximation, with radiation equilibrium, the fluxes obey the equations

$$dq^+/d\tau = -\beta(q^+ - q^-) \tag{17a}$$

$$-dq^-/d\tau = -\beta(q^- - q^+) \tag{17b}$$

where q^+ and q^- are the radiant heat flux in the forward and backward directions, respectively. Equations (15), (18), and (19) define the extinction coefficient, the optical depth, and the albedo:

$$d\tau = \sigma_e\, dx \tag{18}$$

$$\omega = \sigma_s/\sigma_e \tag{19}$$

The term

$$\beta = 1 - \omega + 2\omega b \tag{20}$$

depends on the backscattered fraction factor b.

The radiant heat flux is given by the equation

$$q = \sigma^0(T_1^4 - T_2^4)/(1 + \beta\tau_0) \tag{21}$$

5.4. Linear Anisotropic Scattering (LAS) Model

The LAS model has been developed by Dayan and Tien [15]. This model is valid for spherical particles. The phase function corresponding to the scattering by one spherical particle has the form $(1 + a_1 \cos\theta_0)/4$, where θ_0 is the scattering angle and a_1 is the angular distribution coefficient characterizing forward–backward scattering. The coefficients a_1 and b satisfy the equation

$$a_1 = 2(1 - 2b) \tag{22}$$

The expression of the radiant heat flux is

$$q = \sigma^0(T_1^4 - T_2^4)/(1 + \gamma\tau_0) \tag{23}$$

where

$$\gamma = (3 - \omega a_1)/4 \tag{24}$$

for isotropic scattering, $b = 0.5$, $a = 0$, and $\gamma = 3/4$.

The factors b, a_1, σ_s, and σ_a have to be known. Their calculation requires the knowledge of the complex refractive index, the size distribution of particles, and the volume fraction. Tong and Tien [14] carried out such a calculation in the case of silicate and pure silica fibers, assuming that the scattering by the cylindrical fibers is approximated by the one of some equivalent spheres. As illustrated in Fig. 15 the b factor oscillates as a function of wavelength; moreover, it depends on the radius of the fibers. A wavelength average b factor is still a function of the radius, decreasing from 0.4 to 0.3 when the radius increases from 1 to 4 μm. As the radius of the fibers increases, the forward scattering increases.

Equations (21) and (23) are very similar in form. In the optically thick approximation and isotropic scattering, these equations lead to Eqs. (13) and (16), respectively.

The important difference between the models is that the anisotropic models TF and LAS contain informations describing the scattering pattern of the fibers, by means of the factors b and a_1.

The isotropic models give a wrong expression of the radiant heat flux when the optical thickness is small. According to the optically thick approximation, some values of $q/\sigma^0(T_1^4 - T_2^4)$ given by the different models are reported in Table I, for $\omega = 0.6$ (value computed by Tong and Tien).

It should be noted that the S-S and M-E models are not valuable for the optically thin approximation. In this optically thin approximation, the

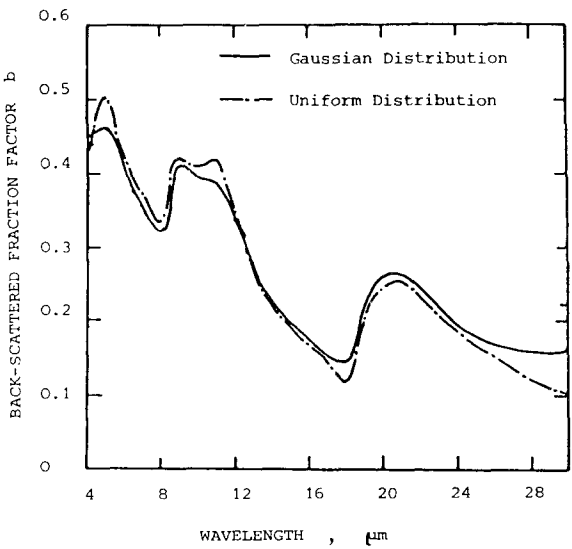

Fig. 15. Typical backscattering fraction factor for a silicate fibrous insulation [14].

Table I. Some Values of $q/\sigma^0(T_1^4 - T_2^4)$ Given by Different Models

	Model			
	S-S	M-E	TF	LAS
$q/\sigma^0(T_1^4 - T_2^4)$	$1/\tau_0$	$4/3\tau_0$	$1/(1+\beta\tau_0)$	$1/(1+\gamma\tau_0)$
Optically thick approximation: $\tau_0 \gg 1$				
$q\tau_0/\sigma^0(T_1^4 - T_2^4)$	1	4/3	$1/\beta$	$1/\gamma$
Isotropic: $b = 0.5$	1	1.33	1	1.33
Anisotropic: $b = 0.3$	1	1.33	1.32	1.59

difference between TF and LAS models should become less important, as seen in Eqs. (21) and (23).

It appears to be very difficult to compute the parameters such as σ_e, β, and γ, so that the comparison of the different models is not really convincing. As an illustration of this comparison, Fig. 16 shows the case of a glass-fiber insulating material [14]. By using the calculated value of σ_e an agreement with the experimental data is not obtained, by the way an empirical value of σ_e has to be used. Thus it is difficult to say what model gives the best agreement with the experimental data.

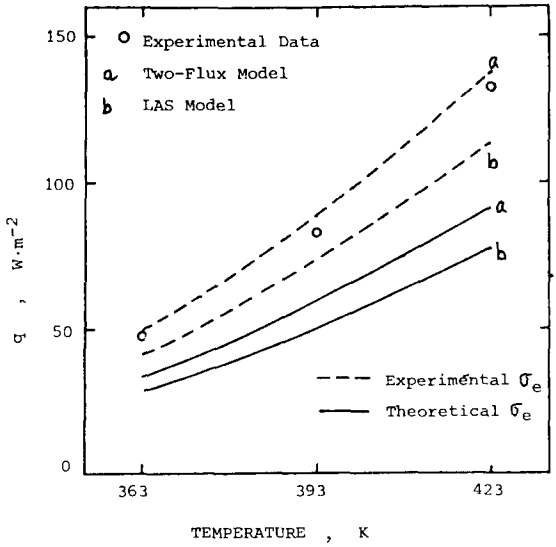

Fig. 16. Radiative heat transfer in a glass-fiber insulation. Comparison of the experimental data and different models [14].

To compute σ_e, the values of σ_a and σ_s are needed. When σ_a is known, a method to get σ_s is to measure the diffuse reflectivity ρ_∞ with a sample of infinite thickness and to calculate σ_s from the function

$$\sigma_a/\sigma_s = (1-\rho_\infty)^2/4\rho_\infty \tag{25}$$

The accuracy of this method is sometimes sufficient [16, 17], compared to the uncertainties introduced in the theoretical computation of σ_s. By the way, the simplest model of Schuster and Schwarzchild may be the best one, in the optically thick approximation. It can explain how the thermal conductivity of some alumina ceramics increases above 1500 K [16].

6. CONCLUSIONS

The radiative heat transfer in fibrous insulating materials and in porous ceramics depends on the infrared properties of the absorbing and scattering medium. Several models have been proposed to calculate the radiant heat flux. They are more or less elaborated, but all of them need the knowledge of at least the absorption and scattering coefficients. The calculation of the optical parameters, such as the absorption σ_a and scattering σ_s coefficients, backscattered fraction factor b, and scattering phase function parameter a_1, has been carried out by several authors, but it needs such drastic approximations that it seems better to use a value of the scattering coefficient σ_s obtained from the measurement of the diffuse reflectivity of an infinite thick sample. Due to the uncertainties in the calculation of these coefficients, the experimental data of absorption are useful.

The infrared absorption can be obtained by transmission measurements in single crystals. It has been shown in the case of Al_2O_3 and MgO that the analysis of absorption data as a function of temperature gives the possibility of decomposing the lattice absorption coefficient on its different multiphonon contributions. The study of multiphonon components is necessary to understand as well as to predict the frequency and temperature behavior of the lattice absorption in materials. Measurements on TiO_2 and ZrO_2 also have been reported; it has been observed that electronic effects considerably enhance the absorption level at high temperatures.

ACKNOWLEDGMENT

The authors thank J. F. Sacadura (INSA, Lyon, France) for valuable information and discussions on radiative heat transfer.

REFERENCES

1. F. Gervais, *Infrared and Millimeter Waves, Vol. 8* (Academic Press, New York, 1983).
2. D. Billard, K. Dembinski, and A. M. Anthony, *Rev. Phys. Appl.* **14**:977 (1979).
3. D. Billard and B. Piriou, *Mat. Res. Bull.* **9**:943 (1974).
4. B. Bendow, H. G. Lipson, R. N. Brown, R. C. Marshall, D. Billard, and S. S. Mitra, *J. Phys. Coll. C6* **42**:140 (1981).
5. B. Bendow, *Solid State Phys.* **33**:249 (1978).
6. D. Billard, F. Gervais, and B. Piriou, *Phys. St. Sol.* **75b**:117 (1976).
7. F. Gervais, B. Piriou, and F. Cabannes, *J. Phys. Chem. Solids* **34**:1785 (1973).
8. F. Gervais, D. Billard, and B. Piriou, *Rev. Int. Hautes Temp. Refract.* **12**:58 (1975).
9. D. Billard, Private communication.
10. D. Billard, J. Simonato, and B. Piriou, *High Temp. High Press.* **8**:437 (1976).
11. D. Billard, F. Gervais, and B. Piriou, *Int. J. Infrared Millimeters Waves* **1**:641 (1980).
12. R. Siegel and J. R. Howell, *Thermal Radiation Heat Transfer* (McGraw–Hill, New York, 1972).
13. B. Larkin and S. Churchill, *AIChE J.* **5**:467 (1959).
14. T. W. Tong and C. L. Tien, *Trans. ASME* **105**:70 (1983).
15. A. Dayan and C. L. Tien, *J. Q. SRT* **16**:113 (1976).
16. F. Cabannes, *High Temp. High Press.* **8**:155 (1976).
17. F. Cabannes, *Rev. Int. Hautes Temp. Refract.* **17**:120 (1980).